RP Current Trends In Engineering And Technology
Vol. 3, No. 4 (October – December 2024) pp. 80–85
e-ISSN: 2583-5491

RESEARCH PLATEAU PUBLISHERS

Cite this article: Ajit Singh, High-intensity helicon wave-induced stimulated Brillouin scattering in magnetized piezoelectric semiconductors, *RP Cur. Tr. Eng. Tech.* **3** (2024) 80–85.

Original Research Article

High-intensity helicon wave-induced stimulated Brillouin scattering in magnetized piezoelectric semiconductors

Ajit Singh*
Assistant Professor, Department of Physics, Government College, Kalka – 133302 (Panchkula) Haryana, India
*Corresponding author, E-mail: ajitnehra2010@gmail.com

ARTICLE HISTORY
Received: 03 Oct. 2024
Revised: 18 Dec. 2024
Accepted: 21 Dec. 2024
Published online: 24 Dec. 2024

KEYWORDS
Stimulated Brillouin scattering; Helicon wave; Magnetized plasma; Growth rate; Threshold intensity; Semiconductor.

ABSTRACT
A comprehensive analytical study is carried out on the stimulated Brillouin scattering (SBS) of a high-intensity helicon pump wave traveling parallel to an applied magnetic field within an n-type cubic piezoelectric semiconducting plasma of a specific symmetry class. Using a hydrodynamic approach for a uniform, piezoelectric, single-component (electron) semiconducting plasma, a general dispersion relation is derived. The study examines the threshold values of the pump electric field and the initial growth rates of the excited modes, considering both left-hand and right-hand circularly polarized waves when the pump exceeds the threshold. Numerical evaluations are performed for n-type indium antimonide (n-InSb) at 77 K subjected to a high-power helicon wave. The laser field intensities considered range from 10^7 to 10^{11} Wm^{-2}, which are assumed to remain below the damage limit of the InSb crystal, and the wave amplitudes are within experimentally achievable levels.

1. Introduction

Driven by the growing interest in stimulated Brillouin scattering (SBS), this paper presents the results of an analytical study on Brillouin instability in a longitudinally magnetized piezoelectric semiconducting plasma exposed to a high-power helicon pump wave. The work also explores the conditions under which the unstable Brillouin mode can grow within the crystal.

In general, the dielectric constant of a scattering medium is influenced by its primary excitations, such as molecular vibrations or acoustic and optical phonons, which enable the coupling of an incident light wave with these excitations. In a semiconducting plasma, a time-dependent electric field induces a corresponding electrostrictive strain, which generates an acoustic wave in the medium. This interaction between the electromagnetic wave and the acoustic wave leads to the phenomenon of stimulated Brillouin scattering (SBS). The scattered wave can propagate in various directions, but the intensity is maximized in the backward direction, accompanied by a characteristic frequency shift equal to the acoustic frequency [1]. The theoretical foundations of SBS were first developed by Kroll [2] and Tang [3], and later reviewed by Starunov [4] and Fabelinskii [5]. Singh et al. [6] provided a simplified analytical approach to analyze the influence of piezoelectricity and magnetic field on stimulated Brillouin scattering. Experimentally, Asam et al. [7] observed SBS in germanium using a pulsed CO_2 laser, while Winterling [8] and colleagues utilized SBS-generated ultrasonic waves in the microwave range to study ultrasonic absorption in quartz at 29 GHz. Sussman and Ridley [9] reported measurements of amplified acoustic flux in oxygen-doped n-GaAs crystals using a continuous-wave Nd:YAG laser (1.06 μm). More recently, Huey et al. [10] demonstrated experimental SBS in microwave-plasma interactions.

A survey of the literature indicates that no studies have yet explored the conditions required to achieve amplified acousto-helicon flux in a solid medium irradiated by a high-power helicon pump wave. The nonlinear excitation of acousto-helicon waves in piezoelectric semiconducting plasmas has been a highly active area of research due to its significant applications in semiconductor diagnostics and device technology [11–14]. Recently, Kumar et al. [15] analyzed the influence of piezoelectricity, doping and magnetostatic field on Brillouin amplification in compound ($A^{III}B^{V}$ and $A^{II}B^{VI}$) semiconductors. The present study focuses on an analytical investigation of stimulated Brillouin scattering (SBS) and the resulting instability of acousto-helicon waves in a homogeneous, nondegenerate n-type (electron-only) piezoelectric semiconductor exposed to a high-power helicon pump wave. The model considers a cubic piezoelectric crystal of the symmetry class $\bar{4}3m$ subjected to a strong longitudinal magnetostatic field $\vec{B}_s$ along the z-axis, parallel to the electric field $\vec{E}_0$ of the high-amplitude helicon pump wave $E_0 \exp[i(\omega_0 t - k_0 z)]$. The scattered electromagnetic and transverse acoustic waves, denoted by $(\omega_1, \vec{k}_1)$ and $(\omega, \vec{k})$ respectively, also propagate along the z-direction. These waves satisfy the energy and momentum conservation conditions: $\omega_1 = \omega_0 - \omega$ and $\vec{k}_1 = \vec{k}_0 - \vec{k}$. The analysis employs the coupled-mode theory, previously used by Kumar et al. [15] for a simplified treatment of SBS.

However, the current study has been carried out under the following assumptions [16-19]:

(i) The amplitude of the pump electric field is assumed to remain below the damage threshold of the crystal under consideration.
(ii) Nonlinear material effects, which are significant in strongly piezoelectric materials like $LiNbO_3$, are neglected by focusing on moderately piezoelectric semiconductors, such as III-V binary compounds.
(iii) The semiconductor is assumed to have an isotropic and nondegenerate conduction band.
(iv) Band non-parabolicity, which contributes approximately 3% deviation from a parabolic band structure, is neglected.
(v) Electron concentrations are taken such that the electron plasma frequency is sufficiently large and nearly matches the pump frequency.
(vi) The pump wave vector $\vec{k}_0$ is assumed to be approximately twice that of the acoustic wave vector $k\,(k_0 \approx 2k)$.

Therefore, the present analysis is well-suited for studying SBS in n-type heavily doped III-V semiconductors, such as n-InSb and n-GaAs, when irradiated with a high-power circularly polarized electromagnetic wave. In this study, the dispersion relation is solved for complex frequencies $\omega(=\omega_r + i\omega_i)$ with real positive values of the wave vector k throughout the analysis. A propagating mode is considered unstable and growing only when ω_i is less than zero with $|\omega_i|$, representing the initial growth rate of the unstable mode. Detailed numerical evaluations have been carried out to determine conditions for the onset of Brillouin instability and the initial growth rates of unstable acousto-helicon modes at pump field amplitudes significantly above threshold, specifically for n-InSb at 77 K.

2. Dispersion relation

We adopt a hydrodynamic model for a homogeneous, single-component (electron) piezoelectric semiconducting plasma, following the geometrical configuration described in Section 1. The time-dependent electric field $\vec{E}_0$ of the pump wave induces an electrostrictive strain in the medium, which generates an accompanying acoustic wave. This acoustic wave modulates the optical dielectric constant, enabling energy exchange between the acoustic wave and the electromagnetic wave, whose frequency is approximately equal to that of the acoustic wave. Consequently, applying the frequency-matching condition $\omega_1 = \omega_0 - \omega$, yields the relation $\omega_0 \approx 2\omega$. The resulting net electrostrictive force per unit volume is given by [1].

$$\vec{F} = \frac{1}{2}\Gamma\vec{\nabla}E^2 . \tag{1}$$

Here, Γ denotes the change in the optical dielectric constant, which is approximately 10^{-11} Fm^{-1}.

We assume that the internally generated acoustic wave is a pure shear wave propagating along the z-axis, which corresponds to the (001) cubic axis of the crystal. The lattice displacement occurs along the x- and y-axes, representing a transverse sound wave, corresponding to the (110) and (11$\bar{}$0) cubic axes, respectively. The analysis considers a cubic piezoelectric III-V binary semiconducting crystal of a specific symmetry class. For the propagation of low-frequency acoustic vibrations in a piezoelectric crystal, the lattice's electric and elastic properties are coupled; thus, the polarization and accompanying electric field must be taken into account. The piezoelectric characteristics of the material are described by the elements e^{ijk} of its piezoelectric tensor [20]. It is well established that cubic crystals of class $\bar{4}3m$ possess only a single independent piezoelectric constant [21], e_{14}. Consequently, the lattice equation of motion, including the electrostrictive force (as given in (1)) and under the condition $u_z = 0$, can be expressed as follows:

$$\rho\frac{\partial^2 u_x}{\partial t^2} = C_{44}\frac{\partial^2 u_x}{\partial z^2} + e_{14}\frac{\partial E_x}{\partial z} + \frac{\Gamma}{2}\frac{\partial E^2}{\partial z} \tag{2a}$$

and

$$\rho\frac{\partial^2 u_y}{\partial t^2} = C_{44}\frac{\partial^2 u_y}{\partial z^2} - e_{14}\frac{\partial E_y}{\partial z} + \frac{\Gamma}{2}\frac{\partial E^2}{\partial z} . \tag{2b}$$

Here, ρ represents the crystal density, C_{44} is the relevant elastic stiffness constant, and e_{14} denotes the piezoelectric stress constant. The other fundamental equations employed in this analysis are as follows:

$$\frac{\partial\vec{v}_0}{\partial t} + (\vec{v}_0.\vec{\nabla})\vec{v}_0 + \nu\vec{v}_0 = \frac{e}{m}[\vec{E}_0 + (\vec{v}_0 \times \vec{B}_0)] \tag{3}$$

$$\frac{\partial\vec{v}}{\partial t} + (\vec{v}_0.\vec{\nabla})\vec{v} + \nu\vec{v} = \frac{e}{m}[\vec{E} + (\vec{v} \times \vec{B})] - \frac{k_B T}{mn_0}\vec{\nabla}n \tag{4}$$

$$\frac{\partial n}{\partial t} + (\vec{v}_0.\vec{\nabla})n + n_0(\vec{\nabla}.\vec{v}) = 0 \tag{5}$$

$$\frac{\partial\vec{E}}{\partial z} = \frac{en}{\varepsilon} - \frac{e_{14}}{\varepsilon}\frac{\partial^2\vec{u}}{\partial z^2} \tag{6}$$

$$\vec{\nabla}\times\vec{E} = -\frac{\partial\vec{B}}{\partial t} \tag{7}$$

$$\vec{\nabla}\times\vec{H} = \vec{J} + \frac{\partial\vec{D}}{\partial t} \tag{8}$$

$$\vec{D} = \varepsilon\vec{E} + \vec{P} \tag{9}$$

$$\vec{P} = -\Gamma\vec{E}\frac{\partial\vec{u}}{\partial z} . \tag{10}$$

Equations (3) and (4) represent the zero- and first-order momentum transfer relations, where $\vec{v}_0$ and $\vec{v}$ denote the oscillatory electron fluid velocities induced by the electric fields of the pump and scattered waves, respectively. $\vec{B}_0 = \vec{k}_0 \times \vec{E}_0 / \omega_0$ is the oscillatory magnetic field of the incident laser radiation. Equation (5) is the continuity equation, with n_0 and n representing the unperturbed and perturbed electron densities, respectively. These expressions are valid for non-degenerate semiconductors. T is the electron temperature, which is approximated to be equal to the lattice temperature,

and k_B is the Boltzmann constant. In Equations (3) and (5), electrons are assumed to have a scalar effective mass. Equation (6) is the Poisson equation, modified to include the piezoelectric contribution.

Following the approach of Byer [22] and using Equations (7)–(10), the general wave equation can be expressed as:

$$\vec{\nabla}\times\vec{\nabla}\times\vec{E} = -\mu_0\frac{\partial\vec{J}}{\partial t} - \frac{1}{c_L^2}\frac{\partial^2\vec{E}}{\partial t^2} + \mu_0\Gamma\left(\vec{E}\frac{\partial\vec{u}}{\partial z}\right), \tag{11}$$

where $\vec{J}$ represents the perturbed current density, which is defined as:

$$\vec{J} = n_0 e\vec{v} + ne\vec{v}_0 . \tag{12}$$

Here, $c_L(=\varepsilon_0\varepsilon_L\mu_0)^{-1/2}$ denotes the velocity of the electromagnetic wave in the lattice. The quantity $\vec{v}_0$ is derived from Equation (3) by assuming that the pump wave is proportional to $\exp[i(\omega_0 t - \vec{k}_0.\vec{r})]$, giving:

$$v_{0\pm} = -i\frac{e}{m}\frac{\bar{\omega}_0}{\omega_0}(\bar{\omega}_0 - i\nu \pm \omega_c)^{-1}E_{0\pm}, \tag{13}$$

where $v_{0\pm} = v_{0x} \pm iv_{0y}$, $E_{0\pm} = E_{0x} \pm iE_{0y}$,

and $\bar{\omega}_0 = \omega_0 - \vec{k}_0.\vec{v}_0$, $\omega_c = eB_s/m$.

We assume that the low-frequency perturbations vary proportionally with $\exp[i(\omega t - kz)]$. Following the method of Kumar et al. [15] and employing Equations (1)–(10) in the collision-dominated regime ($\nu >> \omega; \vec{k}.\vec{v}_0; \vec{k}_0.\vec{v}_0$), one obtains:

$$\frac{\partial^2 n}{\partial t^2} + \nu\frac{\partial n}{\partial t} + k^2 v_{th}^2 n \mp \delta_1 n + \delta_2 u_{\mp} = i(k+k_0)\bar{E}_0 n . \tag{14}$$

Here $\delta_1 = \dfrac{\omega_p^2\omega_0\bar{\omega}}{\omega(\bar{\omega} - i\nu \mp \omega_c)} - \dfrac{\omega_p^4\bar{\omega}^2}{\omega(k^2c_L^2 - \omega^2)(\bar{\omega} - i\nu \mp \omega_c)}$,

$\delta_2 = \dfrac{n_0 e e_{14}}{m\varepsilon}\dfrac{k^2\omega\bar{\omega}}{(k^2c_L^2 - \omega^2)}$, $\bar{E}_0 = \dfrac{e}{m}\left(\dfrac{\bar{\omega}_0}{\omega_0}\right)E_{0\pm} - \omega_c v_0$,

$\bar{\omega} = \omega - \vec{k}.\vec{v}_0$, $\omega_p = \left(\dfrac{n_0 e^2}{m\varepsilon_0\varepsilon_L}\right)^{1/2}$ (plasma frequency)

and $v_{th} = \left(\dfrac{k_B T}{m}\right)^{1/2}$ (electron thermal velocity).

In deriving Eq. (14) we have taken $u_{\pm} = u_x \pm iu_y$, $v_{\pm} = v_x \pm iv_y$, $B_{\pm} = B_x \pm iB_y$, and $E_{\pm} = E_x \pm iE_y$, where + and – signs correspond to the right- and left-hand circular polarizations, respectively. The following relations were used in the derivation:

$$v_{\pm} = -\left(\frac{ie}{m}\right)\left(\frac{\bar{\omega}}{\omega}\right)(\bar{\omega} - i\nu \mp \omega_c)^{-1}, \tag{15}$$

$$i\left(\frac{k^2}{\mu_0\omega} - \varepsilon\omega\right)E_{\pm} = n_0 e v_{\pm} - k\omega e_{14}u_{\mp} . \tag{16}$$

Equation (15) is obtained from Equation (4), while Equation (16) follows from Equation (8).

Physically, the high-frequency pump wave excites a low-frequency acoustic wave in the medium, leading to high- and low-frequency components of the carrier density fluctuations, denoted by n_f and n_s, and perturbed electron fluid velocities, v_f and v_s, oscillating at the frequencies $\omega_1(=\omega_0 \pm \omega)$ and ω of the generated electromagnetic and acoustic waves, respectively.

Based on the discussion above, Equation (14) can be expressed as:

$$\frac{\partial^2 n_f}{\partial t^2} + \nu\frac{\partial n_f}{\partial t} + \omega_R^2 n_f = i(k+k_0)\bar{E}_0 n_s \tag{17}$$

and

$$\Omega^2 + \frac{n_0 e e_{14}}{m\varepsilon}\frac{k^2\omega\bar{\omega}}{(k^2c_L^2 - \omega^2)}u_{\mp} = i(k+k_0)\bar{E}_0 n_f , \tag{18}$$

where

$$\Omega^2 = \omega_R^2 + i\nu\omega + \frac{\omega_p^4\bar{\omega}^2}{\omega(k^2c_L^2 - \omega^2)(\bar{\omega} - i\nu \mp \omega_c)},$$

$$\omega_R^2 = k^2 v_{th}^2 + \frac{\omega_p^2\bar{\omega}}{\omega} .$$

The quantity n_f contains components at frequencies $\omega_0 \pm \omega$. Higher-order components $\omega_0 \pm b\omega$ (b > 1) are negligible because they are non-resonant, unlike the primary component $\omega_0 \pm \omega$, which satisfies the resonance condition $\omega << \omega_c \approx \omega_p$. Thus, Equation (17) can be expressed for the two main components of n_f as:

$$n_f = i(k+k_0)\bar{E}_0 n_s[\{\omega_R^2 - (\omega_0+\omega)^2 + i\nu(\omega_0+\omega)\}^{-1} + \{\omega_R^2 - (\omega_0-\omega)^2 + i\nu(\omega_0-\omega)\}^{-1}]. \tag{19}$$

Assuming $\omega_0 \approx \omega_R(\approx \omega_p)$ and $\omega << \omega_0$, Equation (19) reduces to:

$$n_f = -\frac{i(k+k_0)\bar{E}_0 n_s}{\omega_R^2}\left[\frac{\omega_R}{(\omega + \delta - i\nu)} - \frac{\omega_R}{(\omega - \delta - i\nu)}\right], \tag{20}$$

where $\delta = \omega_0 - \omega_R$.

By applying Equations (1) and (6), we obtain:

$$n_s = \left[\left\{\omega^2 - k^2c_t^2 - \frac{e_{14}k^2}{\varepsilon\rho}\left(e_{14} - \frac{\Gamma E_0}{2}\right)\right\}\left\{\frac{e}{\varepsilon\rho}\left(e_{14} - \frac{\Gamma E_0}{2}\right)\right\}\right]u \tag{21}$$

Here, $c_t = (C_{44}/\rho)^{1/2}$ represents the acoustic velocity in the crystal. Equation (8) can be used to express $u_{\pm}$ in terms of $E_{\pm}$ as:

$$u_{\mp} = \frac{J_{\pm}}{k\omega e_{14}} - \frac{i}{k\omega e_{14}}\left\{\frac{k^2}{\mu_0\omega_1 - \varepsilon\omega_1}\right\}E_{\pm}. \quad (22)$$

Combining Equations (12), (15), and (20)–(22) gives the components of $\vec{J}$ as:

$$J_{\pm} = \frac{\varepsilon}{(1-Q)}\left[\frac{\omega_p^2\bar{\omega}_1^2}{\omega_1(\bar{\omega}_1^2 - i\nu\mp\omega_c)} - \frac{iQ}{\omega_1}(k^2c_L^2 - \omega_1^2)\right]E_{\pm}, \quad (23)$$

where $\bar{\omega}_1 = \omega_1 - \vec{k}.\vec{v}_0$ and

$$Q = \frac{v_{0\pm}\varepsilon\rho Z_1}{\omega k e_{14}}\left\{1 - \frac{2i\delta(k+k_0)\bar{E}_0}{\omega_R(\nu^2+\delta^2)}\right\}, \quad (24)$$

in which

$$Z_1 = \frac{\omega^2 - k^2c_t^2 - \frac{k^2e_{14}}{\varepsilon\rho}\left(e_{14} - \frac{\Gamma E_0}{2}\right)}{\left(e_{14} - \frac{\Gamma E_0}{2}\right)}$$

and have assumed $E_{\pm} >> \frac{k^3v_{th}^2}{\omega_p^2}\frac{e_{14}}{\varepsilon}u_{\mp}$.

We now consider the general wave equation (11), which describes the scattered transverse electromagnetic wave with frequency $\omega_1(\approx\omega_0)$ and wave number k_1, varying as $\exp[i(\omega_1 t - k_1 z)]$. Under the specified configuration, Equation (11) simplifies to:

$$-k_1^2E_{\pm} + i\omega_1\mu_0 J_{\pm} + \frac{\omega_1^2}{c_L^2}E_{\pm} = -\mu_0\Gamma\frac{\partial^2}{\partial t^2}\left(E_{\pm}\frac{\partial u_{\mp}}{\partial z}\right). \quad (25)$$

Following the approach of Yariv [1], and employing Equations (6) and (21), Equation (1) can be expressed as:

$$u_{\pm} = -ik\left(e_{14} - \frac{\Gamma E_0}{2}\right)(\omega^2 - k^2c_t^2)^{-1}E_{\mp}. \quad (26)$$

Substituting Equations (23) and (26) into (25) and performing the necessary mathematical simplifications leads to the general dispersion relation describing the stimulated Brillouin scattering (SBS) phenomenon:

$$\left[k_1^2c_L^2 - \omega_1^2 + i\frac{\omega_1\Delta}{(1-Q)} + \frac{\mu_0\Gamma k^2c_L^2\omega_1^2E_0\left(e_{14} - \frac{\Gamma E_0}{2}\right)}{\rho(\omega^2 - k^2c_t^2)}\right]E_{\pm} = 0, \quad (27)$$

where $\Delta = \frac{\omega_p^2\bar{\omega}_1}{\omega_1(\bar{\omega}_1 - i\nu\mp\omega_c)} - i\frac{Q}{\omega_1}(k_1^2c_L^2 - \omega_1^2)$.

Equation (27) describes two independent circularly polarized modes, corresponding to E_+ (right-hand) and E_- (left-hand) polarizations. This circular polarization arises from the coupling of two transverse, linearly polarized modes due to the presence of a finite longitudinal magnetostatic field B_s. In the absence of B_s, the system reduces to the conventional SBS of transverse waves. Under such conditions, the dispersion relation can be analyzed to explore the possibility of SBS and the resulting Brillouin instability in n-type piezoelectric semiconducting plasmas. However, since our focus is on circularly polarized waves, we consider Equation (27) in the presence of the magnetostatic field.

3. Growth rate and threshold field

In the slow-wave limit, applying the quasi-static approximation $(k_1^2c_L^2 >> \omega_1^2)$ allows us to simplify the dispersion relation, which can then be expressed as:

$$(\omega^2 - k^2c_t^2)\frac{k_1^2c_L^2 \pm i\omega_p^2\bar{\omega}_1}{(1-Q)\omega_c} = -\frac{\mu_0\Gamma k_1^2c_L^2\omega_1^2E_0}{\rho}\left(e_{14} - \frac{\Gamma E_0}{2}\right). \quad (28)$$

From the above equation, it is evident that the shear acoustic and transverse electromagnetic waves—obtained by setting the first and second factors on the left-hand side to zero, respectively—are coupled through the nonlinear electrostrictive force in the piezoelectric semiconducting plasma. The presence of a high-power pump with amplitude $E_0 \neq 0$ is a necessary condition for this coupling, as clearly indicated by the equation.

We now turn to the main focus of this work: the possibility of stimulated Brillouin scattering (SBS) and the Brillouin instability of acousto-helicon waves under a high-power helicon field. The dispersion relation (28) is solved for complex $\omega(=\omega_r + i\omega_i)$ with real positive values of k, such that $\omega_r = kc_t$. By equating the imaginary parts, one obtains:

$$\omega_i = \mp\left[(1-Q)\left(e_{14} - \frac{\Gamma E_0}{2}\right)\left(\frac{\omega_c k c_L^2\omega_1\mu_0\Gamma}{2c_t\rho\omega_p^2\varphi}\right)E_{0\pm}\right]. \quad (29)$$

Here, $\varphi = 1 - v_0/c_t$ represents the growth rate. Since v_0, the oscillatory electron fluid velocity from Equation (13), is much greater than the acoustic velocity c_t, it follows that $\varphi < 0$. Therefore, under the condition $\varphi = -|\varphi|$, Equation (29) can be rewritten as:

$$\omega_i = \mp\left[(1-Q)\left(e_{14} - \frac{\Gamma E_0}{2}\right)\left(\frac{\omega_c k c_L^2\omega_1\mu_0\Gamma}{2c_t\rho\omega_p^2|\varphi|}\right)E_{0\pm}\right]. \quad (30)$$

Equation (30) indicates that in the absence of the pump field E_0, the growth rate vanishes. This implies that a finite pump field amplitude is essential for studying SBS, which is a fundamental prerequisite for investigating SBS phenomena. Using the known numerical values of e_{14} and Γ, one can consider $e_{14} >> \Gamma E_0/2$ for a value of E_0 in the range of 10^8 to 10^9 Vm^{-1}. Under these conditions, Equation (30) shows that Brillouin instability occurs only when: (a) $Q > 1$ for the right-hand circularly polarized Brillouin mode, and (b) $Q < 1$ for the

left-hand circularly polarized Brillouin mode, thereby defining the onset of instability at:

$$1-Q=0. \tag{31}$$

By substituting the value of Q into Equation (31), the threshold electric field can be determined as:

$$(E_{0\pm})_{th}=\frac{m}{e}\left(\frac{\omega_0 \mp \omega_c}{\omega_0}\right)\left[\frac{\omega_0\omega_R\nu c_t}{2(k+k_0)}\right]^{1/2}. \tag{32}$$

Equations (30) and (32) can be appropriately applied to various n-type piezoelectric semiconductors that satisfy the assumptions made in their derivation, for the purpose of studying Brillouin instability.

4. Results and discussion

This paper presents an analytical study of the Brillouin instability of acousto-helicon waves under the influence of a high-power helicon pump. The analytical results are applied specifically to n-type InSb at 77 K. The physical constants used in the analysis are as follows:

$$m = 0.014m_0,\ e_{14} = 0.054\ \text{Cm}^{-1},\ \rho = 5.8\times10^3\ \text{kg m}^{-3},$$
$$\varepsilon_L = 17.8,\ \nu = 3.5\times10^{11}\ \text{s}^{-1}.$$

Figure 1 illustrates the variation of the threshold electric fields $(E_{0\pm})_{th}$ with the magnetostatic field ω_c for different wave numbers. From the graph, it is evident that $(E_{0+})_{th}$ decreases as both ω_c, and k increase. However, for other mode, $(E_{0-})_{th}$ increases with ω_c and decreases with increasing k.

Figure 2 shows the dependence of the growth rates $|\omega_{i\pm}|$ on the magnetostatic field (ω_c) for different values of k at E_0 = 5×10^6 Vm^{-1}. The graph indicates that the growth rate of one mode ($|\omega_{i+}|$) is independent of k, while the other ($|\omega_{i-}|$) decreases as k increases. In general, the growth rates of both modes decrease with increasing ω_c, although at higher ω_c values, $|\omega_{i\pm}|$ almost independent of ω_c .

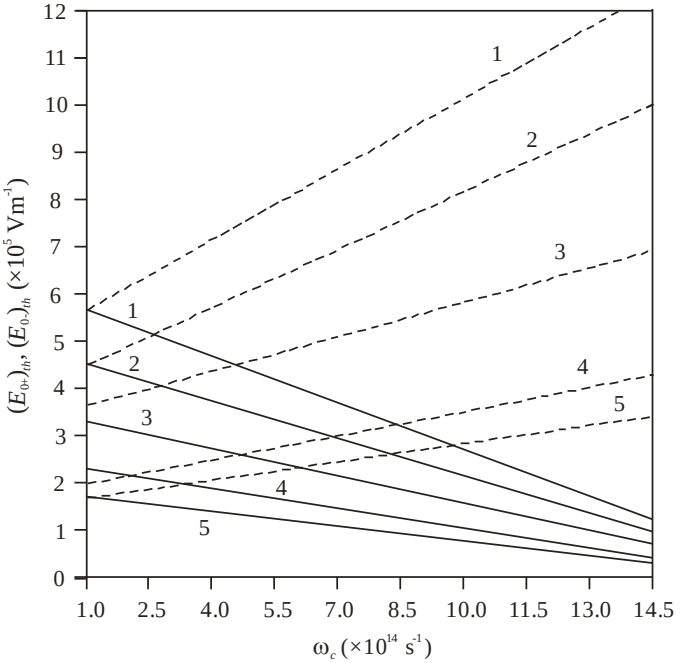

Figure 1: Variation of the threshold pump electric field $(E_{0\pm})_{th}$ with the magnetostatic field ω_c for different wave numbers k: (1) 4×10^5, (2) 8×10^5, (3) 2×10^6, (4) 6×10^6, (5) 10^6 m^{-1}.

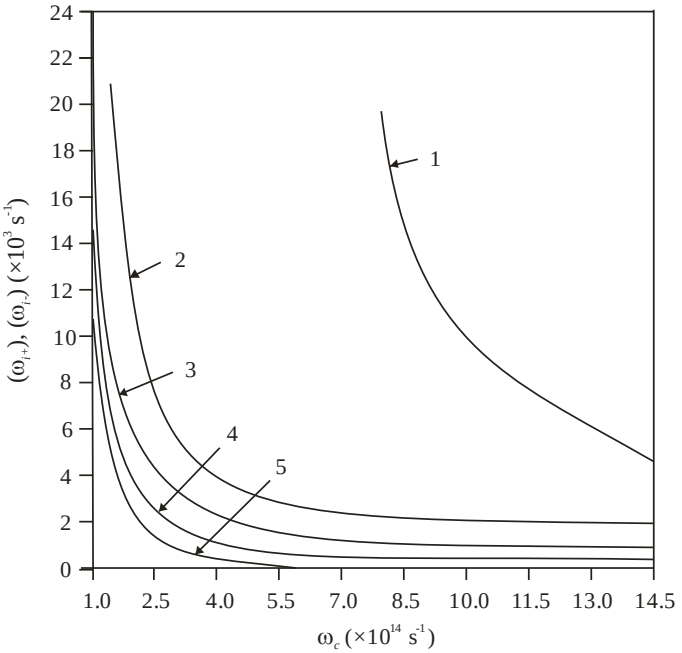

Figure 2: Variation of the growth rates $|\omega_{i\pm}|$ of the excited acousto-helicon waves with the magnetostatic field ω_c for different wave numbers k: (1) 4×10^5, (2) 8×10^5, (3) 2×10^6, (4) 6×10^6, (5) 10^7 m^{-1} at E_0 = 5×10^6 Vm^{-1}.

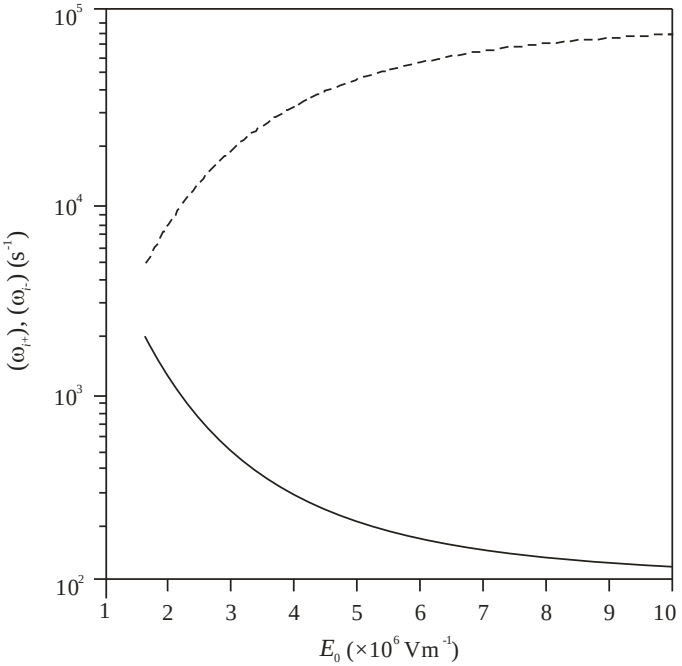

Figure 3: Variation of the growth rates $|\omega_{i\pm}|$ of the excited acousto-helicon waves with the pump electric field amplitude E_0 at ω_c = 2×10^{13} s^{-1} and k = 2×10^6 m^{-1}.

Figure 3 depicts the relationship between the growth rates $|\omega_{i\pm}|$ and the pump field E_0 at ω_c = 2×10^{13} s^{-1} and k = 2×10^6 m^{-1}. It is observed that $|\omega_{i+}|$ increases with E_0 while $|\omega_{i-}|$ decreases. Additionally, higher collision frequencies ν increase the threshold electric fields because greater damping must be overcome for the growth of the excited modes. Higher carrier concentrations reduce the growth rates and increase the threshold field amplitudes. It is also noteworthy that the threshold electric fields and corresponding growth rates are sensitive to the electron effective mass.

The electric field amplitudes considered in this study can be related to the pump intensity I_0 using the expression $I_0 = c_0\varepsilon_0\varepsilon_L|E_0|^2/2\eta$, where η is the refractive index of the crystal (3.9 for InSb) and c_0 is the speed of light in vacuum. The calculations presented here are based on E_0 values ranging from 10^5 to 10^7 Vm^{-1}, corresponding to an intensity range of 6.06×10^7 to 6.06×10^{11} Wm^{-2}. These field strengths can be applied without causing significant damage to the crystal. Such threshold fields are achievable using a high-power helicon source, which is experimentally feasible [23].

5. Conclusions

The results presented in this study indicate that stimulated Brillouin scattering (SBS) and the resulting Brillouin instability of acousto-helicon waves can be achieved in longitudinally magnetized n-type piezoelectric semiconducting plasmas irradiated by a high-power helicon pump wave. Moreover, the plasma parameters in such media can be varied over a wide range with relative ease, allowing for flexible experimental conditions.

References

[1] A. Yariv, *Quantum Electronics*, 2nd ed., John Wiley & Sons, New York (1975) p. 491.

[2] N.M. Kroll, Excitation of hypersonic vibrations by means of photoelastic coupling of high-intensity light waves to elastic waves, *J. Appl. Phys*. **36** (1965) 34.

[3] C.L. Tang, Saturation and spectral characteristics of Stokes emission in stimulated Brillouin process, *J. Appl. Phys*. **37** (1966) 2945.

[4] V.S. Starunov, I.L. Fabelinskii, Stimulated Mandelshtam-Brillouin scattering and stimulated entropy (temperature) scattering of light, *Soviet Phys. - Uspekhi* **12** (1970) 463.

[5] I.L. Fabelinskii, *Quantum Electronics*, Vol. I, Part A, H. Rarbin and C.L. Tang (Ed.), Academic Press, Inc., New York (1975) p. 363.

[6] M. Singh, P. Aghamkar, P.K. Sen, Influence of piezoelectricity and magnetic field on stimulated Brillouin scattering, *J. Nonlin. Opt. Phys. Mater*. **15** (2006) 465–479.

[7] P. Asam, W. Deuflhard, W. Kaiser, Intensity limiting and stimulated Brillouin scattering in germanium, *Phys. Lett. A* **27** (1968) 78.

[8] G.W. Winterling, W. Heiniche, K. Dransfeld, *Light Scattering Spectra in Solids*, G.B. Wright (Ed.), Springer-Verlag, New York (1969) p. 489.

[9] R.S. Sussman, B.K. Ridley, A study of amplified acoustic flux in n-GaAs by Brillouin scattering, *J. Phys. C* **7** (1974) 3941.

[10] H.E. Huey, A. Mase, N.C. Luhmann, Observations of stimulated-Brillouin scattering initiated by ponderomotive force density fluctuations, *Phys. Rev. Lett*. **45** (1980) 795.

[11] V.G. Skobov, E.A. Kaner, Theory of coupled electromagnetic and acoustic waves in metals in a magnetic field, *Soviet Phys. - J. Exper. Theor. Phys*. **19** (1964) 189.

[12] M.C. Steele, B. Vural, *Wave Interactions in Solid State Plasmas*, McGraw Hill Publ. Co., New York (1969) p. 154.

[13] J.S. Yang, H. Zhou, Amplification of acoustic waves in piezoelectric semiconductor plates, *Int. J. Silids Struct*. **42** (2005) 3171-3183.

[14] H.C. Hheih, Transverse phonon-helicon interaction in a semiconductor, *J. Appl. Phys*. **45** (1974) 489-491.

[15] A. Kumar, S. Dahiya, N. Singh, M. Singh, Influence of piezoelectricity, doping and magnetostatic field on Brillouin amplification in compound ($A^{III}B^{V}$ and $A^{II}B^{VI}$) semiconductors, *J. Nonlin. Opt. Phys. Mater*. **30** (2021) 2150010.

[16] R. Kumari, M. Singh, Hot carrier effects on real and imaginary parts of Brillouin susceptibilities of magnetoactive doped III–V semiconductors, *Trends Sci*. **19** (2022) 6185.

[17] P. Kumari, B.S. Sharma, M. Singh, Hot carrier effects on Brillouin susceptibilities of semiconductor magneto-plasmas, *Pramana – J. Phys*. **96** (2022) 49.

[18] D. Singh, B.S. Sharma, M. Singh, Quantum effects on threshold and Brillouin gain characteristics of semiconductor magneto-plasmas, *J. Opt*. **51** (2022) 969–978.

[19] Pravesh, S. Dahiya, N. Singh, M. Singh, Dispersion, threshold and gain characteristics of Brillouin scattered Stokes mode in ion-implanted semiconductor quantum plasmas, *Iran. J. Sci. Technol., Trans A: Sci*. **48** (2024) 757–769.

[20] J.F. Nye, *Physical Properties of Crystals*, Clarendon Press, Oxford (1957).

[21] D.A. Berlincourt. D.R. Curran, H. Jaffe, *Physical Acoustics, Principles and Methods*, Vol. I, Part A, W.P. Mason (Ed.), Academic Press, Inc., New York (1964) p. 169.

[22] R.L. Byer, *Nonlinear Optics*, P.G. Harper and B.S. Wherrett (Ed.), Academic Press, Inc., New York (1977) p. 47.

[23] A.K. Laurinavichus, Yu. K. Pozehela, Nonlinear effects in n-type InSb during propagation of a high-power helicon microwave, *Soviet Phys. - Semicond*. **7** (1974) 1361.